Tide-Topography Interactions: Asymmetries in Internal Wave Generation due to Surface Trapped Currents

Kevin G. Lamb and Michael Dunphy

Department of Applied Mathematics
University of Waterloo
Waterloo, Ontario, Canada
kglamb@uwaterloo.ca

Laboratoire d'Océanographie Physique et Spatiale;
IFREMER Centre de Brest;
ZI Pointe du Diable - CS 10070;
29280 Plouzané, France
mdunphy@uwaterloo.ca

Abstract

The effects of a surface trapped current on the generation of internal waves by periodic flow over a ridge is considered. The currents results in asymmetries in the energy fluxes in the upstream and downstream direction though the total energy flux away from the ridge is not affected by the current. For sufficiently narrow ridges the upstream flux exceeds the downstream flux while the opposite is true for sufficiently wide ridges. The kinetic energy flux makes a significant contribution to the total energy flux and both the work term and the kinetic energy fluxes undergo significant spatial variations while the total energy flux is independent of distance from the ridge.

1 Introduction

The source of approximately half of the internal wave energy in the ocean is tide-topography interactions and the problem of what waves are generated, where they go and where and how they are dissipated has received a lot of attention in recent decades (Egbert and Ray, 2000; Alford, 2003; Niwa and Hibiya, 2004; Simmons et al., 2004; Wunsch and Ferrari, 2004; Garrett and Kunze, 2007). Most work to date has considered a quiescent ocean apart from tidal currents. As quasi-steady currents are a common feature of the world's ocean it is important to understand the impact they have on internal wave generation.

Here, we consider how a steady background current affects the internal wave generation process. Results from fully nonlinear, two-dimensional, non-hydrostatic numerical simulations are described and upstream and downstream energy fluxes are investigated. Rotational affects are not considered so that the current does not have to be geostrophically balanced by a stratification varying in the transverse direction, hence making the problem two-dimensional.

2 Numerical Model and Model Setup

The two-dimensional fully nonhydrostatic Internal Gravity Wave model (Lamb, 1994, 2007) is used in this study to solve the incompressible Euler equations under the Boussi-

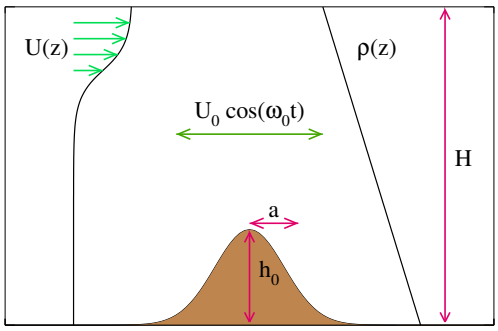

Figure 1: Schematic of the tide-topography interaction problem with a background current.

nesq approximation in a non-rotating reference frame. The model equations are

$$u_t + uu_x + wu_z = -p_x \tag{1a}$$
$$w_t + uw_x + ww_z = -p_z - \rho g \tag{1b}$$
$$\rho_t + u\rho_x + w\rho_z = 0, \tag{1c}$$
$$\vec{\nabla} \cdot \vec{u} = 0. \tag{1d}$$

Here $\vec{u} = (u, w)$ is the velocity in the vertical xz-plane, ρ is the density and p is the pressure, both of which have been scaled by the reference density ρ_0. The rigid lid approximation is used with the surface at $z = 0$. The bottom is at $z = -H + h(x)$ where

$$h(x) = h_0 e^{-\left(\frac{x}{a}\right)^2}. \tag{2}$$

Hence, we consider background currents of the form

$$\bar{U}(z) = \frac{U_s}{4}\Big(1 + \tanh\big(\frac{z - z_s}{d_s}\big)\Big)^2. \tag{3}$$

with z_s and d_s chosen so that the current lies above the ridge (Figure 1). A linear stratification with buoyancy frequency $N = 10^{-3}$ s^{-1} and an M_2 tide with current amplitude $U_0 = 0.05$ m s^{-1} are used.

3 Linear Theory

Following the procedure used by Khatiwala (2003) the linear internal wave field generated by a barotropic tidal flow of frequency ω has the form

$$w(\xi, z, t) = \sum_{\substack{-\infty \\ n\neq 0}}^{\infty} \frac{-in\omega_0}{2\pi} e^{-in\omega_0 t} \int_{-\infty}^{\infty} \hat{h}(k) J_n\Big(\frac{-kU_0}{\omega_0}\Big) \frac{\phi_n(k, z)}{\phi_n(k, -H)} e^{ik\xi}\, dk \tag{4}$$

where the $\phi_n(k, z)$ are solutions of the Taylor-Goldstein equation

$$\mathcal{L}[\phi_n] \equiv \phi_n'' + \left(\frac{N^2(z)}{\big(n\omega_0 - k\bar{U}(z)\big)^2} + \frac{\bar{U}''(z)}{\big(n\omega_0 - k\bar{U}(z)\big)} - 1\right) k^2 \phi_n = 0 \tag{5}$$

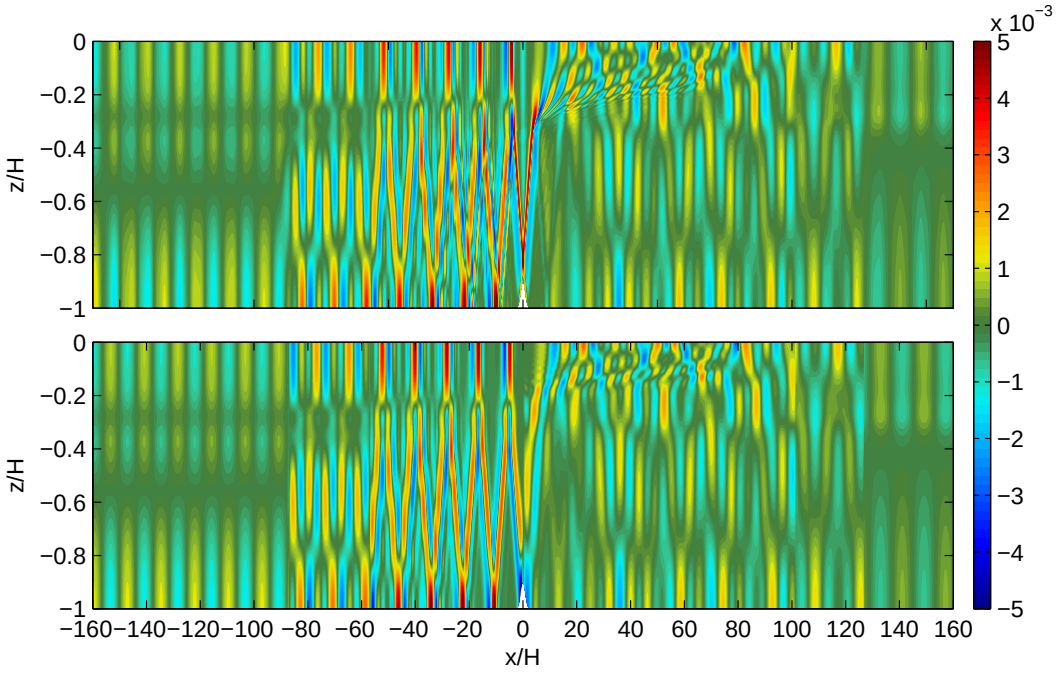

Figure 2: Comparison of wave induced horizontal currents for numerical simulation (upper) and theory (lower) after 15 tidal periods. $h_0/H = 0.1$, $a/H = 1.2$, $(U_s/(NH), z_s/H, d_s/H) = (0.1, -0.3, 0.08)$.

satisfying the boundary conditions

$$\begin{aligned} \phi_n(k,0) &= 0, \\ \phi_n'(k,0) &= 1. \end{aligned} \tag{6}$$

The contributions to the integral are of two types: (i) contributions from the poles where $\phi_n(k,-H) = 0$ and (ii) possibly from the continuous spectrum. Here we do not consider the continuous spectrum as the wave field appears to be well predicted by the discrete spectrum alone which gives the linear internal wave modes. The Taylor-Goldstein equation must be solved numerically so arbitrary stratifications can be considered. Figure 2 compares the theoretical horizontal currents after 15 tidal periods with those from a numerical simulation. For the former the contribution from each mode extends as far as energy moving with the group velocity would reach by this time.

4 Energy Fluxes

The vertically integrated energy flux at a horizontal location x is

$$E_f = KE_f + APE_f + W \tag{7}$$

where

$$\begin{aligned} KE_f &= \int_{-H(x)}^{0} uE_k \, dz, \\ APE_f &= \int_{-H(x)}^{0} uE_a \, dz, \end{aligned} \tag{8}$$

are the vertically integrated kinetic and available potential energy flux densities, and

$$W = \int_{-H(x)}^{0} u p_d \, dz, \tag{9}$$

is the rate work is done by the pressure perturbation p_d. Separating u into the background current plus a perturbation via $u = \bar{U} + u'$ the kinetic energy flux can be split into three pieces (the spatially uniform contribution from $\bar{U}^3$ can be neglected)

$$\begin{aligned} KE_{f1} &= \frac{3}{2} \int_{-H}^{0} \bar{U}^2 u' \, dz, \\ KE_{f2} &= \frac{3}{2} \int_{-H}^{0} \bar{U} u'^2 \, dz, \\ KE_{fr} &= \frac{1}{2} \int_{-H}^{0} \bar{U} w^2 \, dz + \frac{1}{2} \int_{-H}^{0} u'(u'^2 + w^2) \, dz. \end{aligned} \tag{10}$$

In our simulations the 'residual' flux KE_{fr} is negligible. Both the first- and second-order terms KE_{f1} and KE_{f2} can be important. Below we consider fluxes averaged over 4 tidal periods scaled by

$$F_0 = \frac{1}{2} N U_0^2 h_0^2 \tag{11}$$

which is the scaling predicted by linear hydrostatic theory (Simmons et al., 2004; Garrett and Kunze, 2007).

5 Results

We consider a single current with $U_s = 0.5$ m s^{-1}, $z_s = -1500$ m, $d_s = 400$ m and a ridge of amplitude $h_0 = 500$ m in a 5000 m deep ocean. Only the ridge width a is varied.

Figure 3 shows the four largest contributions to the tidally averaged energy flux, along with the total energy flux, as a function of distance from the ridge for the case with $a/H = 1.8$. Values at $t = 20$T are shown. Also shown are the averages of the work term and the total energy fluxes after 40 periods for comparison. There are significant spatial variations in the various contributions to the total flux, however the total flux is independent of distance from the ridge except far from the ridge at $t = 20T$ where higher mode waves have not yet arrived.

Figure 4 shows the total leftward and rightward energy flux as a function of the ridge width a. Comparisons are made with the corresponding fluxes in the case of no background current. For narrow ridges, with $a/H <\approx 3.5$, the upstream (leftward) flux is increased in magnitude by the current while for wider ridges it is decreased. The opposite occurs for the rightward fluxes. For the narrowest ridge the upstream flux is half the downstream flux while for the widest ridge the downstream flux is four times larger than the upstream flux. The total energy flux away from the ridge is the same with and without the background current.

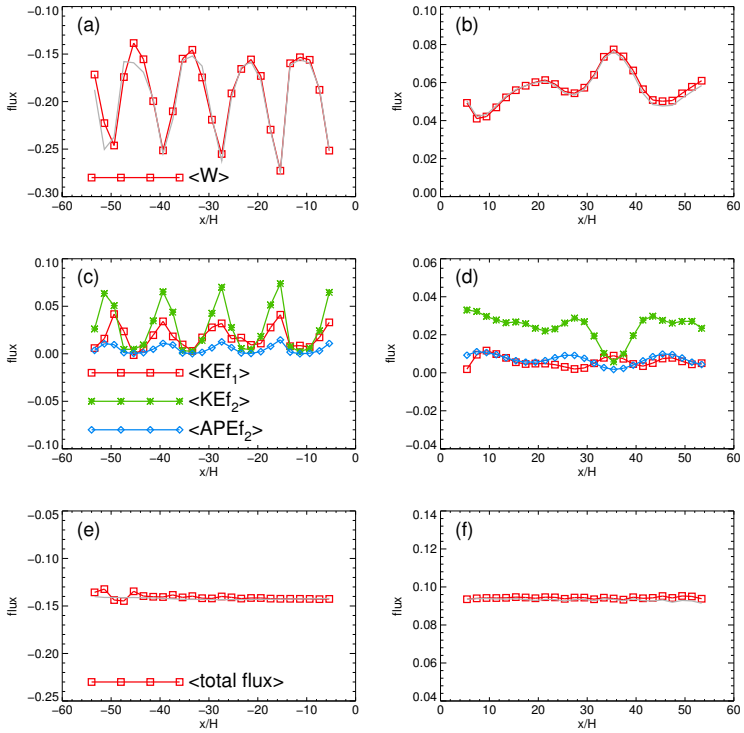

Figure 3: Tidally averaged energy fluxes at $t = 20$T (averaged over previous four periods) scaled by F_0 as a function of distance for case from set 4 with $a/H = 1.8$. Left column shows leftward fluxes, right column shows rightward fluxes. (a,b) $\langle W \rangle$. (c,d) $\langle KE_{f1} \rangle$, $\langle KE_{f2} \rangle$, and $\langle APE_f \rangle$. (e,f) Average of total flux $\langle W + KE_{f1} + KE_{f2} + APE_f \rangle$. In panels (a,b,e,f) the tidally averaged values at $t = 40$T are also shown (grey curves). The range of rightward flux (0.1) values plotted are twice as large as those for the leftward fluxes (0.2).

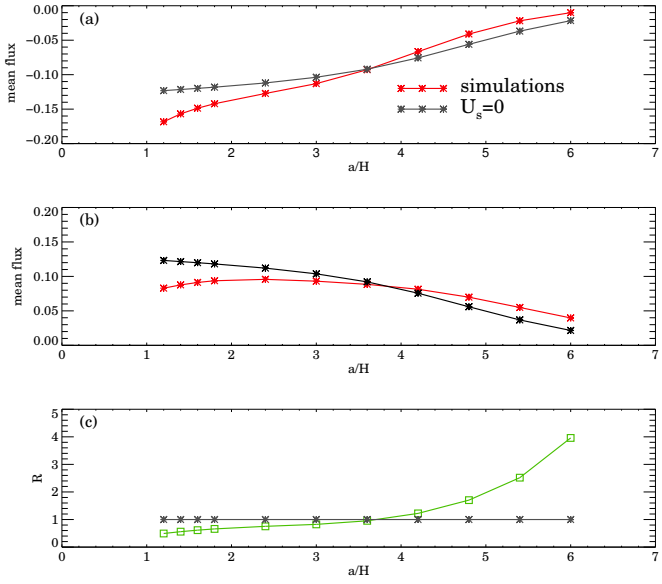

Figure 4: Energy fluxes from fully nonlinear simulations as a function of the ridge width a with and without a background current. Fluxes are scaled by F_0. (a) Leftward (upstream) fluxes. (b) Rightward (downstream) energy fluxes. (c) Ratio of rightward to leftward fluxes. $h_0 = 500$ m, $z_s = -1500$ m, $d_s = 400$ m. The tidal current is 0.05 m s^{-1}.

6 Conclusions

A steady, surface trapped background current introduces an asymmetry into the internal wave generation process, modifying the upstream and downstream energy flux while the total energy flux is unchanged. The upstream energy flux is larger/smaller than the downstream flux for narrow/wide ridges. The kinetic energy flux makes a significant contribution to the total energy flux. There are large spatial oscillations in the work term and the kinetic energy fluxes, particularly in the upstream direction.

References

Alford, M. H. (2003). Redistribution of energy available for ocean mixing by long-range propagation of internal waves. *Nature*, 423.

Egbert, G. D. and Ray, R. D. (2000). Significant dissipation of tidal energy in the deep ocean inferred from satellite altimeter data. *Nature*, 405:775–778.

Garrett, C. and Kunze, E. (2007). Internal tide generation in the deep ocean. *Ann. Rev. Fluid. Mech.*, 39:57–87. doi 10.1146/annurev.fluid.39.050905.110227.

Khatiwala, S. (2003). Generation of internal tides in an ocean of finite depth: Analytical and numerical calculations. *Deep Sea Res.*, 50:3–21.

Lamb, K. G. (1994). Numerical experiments of internal wave generation by strong tidal flow across a finite amplitude bank edge. *J. Geophys. Res.*, 99:843–864.

Lamb, K. G. (2007). Energy and pseudoenergy flux in the internal wave field generated by tidal flow over topography. *Cont. Shelf Res.*, 27:1208–1232.

Niwa, Y. and Hibiya, T. (2004). Three-dimensional numerical simulation of m2 internal tide in the east china sea. *J. Geophys. Res.*, 106(C10). C04027. Doi: 10.1029/2003JC00192.

Simmons, H. L., Jayne, S. R., Laurent, L. C. S., and Weaver, A. J. (2004). Tidally driven mixing in a numerical model of the ocean general circulation. *Ocean Modelling*, 6:245–264.

Wunsch, C. and Ferrari, R. (2004). Vertical mixing, energy, and the general circulation of the oceans. *Ann. Rev. Fluid Mech.*, 36:281–314.